

Temperature Characteristics of Magnetolectric Effect in a Monolithic Langatate-Metglas Heterostructure: The Effect of Annealing

E. Bolotina¹, D. Savelev¹, L. Fetisov¹, A. Turutin², I. Kubasov², A. Temirov², V. Kuts², Y. Qi³, P. Zhou³, A. Klimov¹ and Y. Fetisov^{1,*}

¹MIREA - Russian Technological University, 119454 Moscow, Russia

²National University of Science and Technology MISIS, 119049 Moscow, Russia

³School of Materials Science and Engineering, Hubei University, Wuhan 430062, China

Abstract: Magnetolectric (ME) effects in ferromagnetic-piezoelectric heterostructures manifest themselves as a change in the polarization of the structure in an external magnetic field or a change in magnetization in an electric field. The effects are used to create magnetic field sensors, tunable electronic devices, and new data processing elements. To ensure the thermal stability of these devices, it is important to understand the temperature dependence of the ME effect characteristics. In this paper, we investigated the direct resonant ME effect in a monolithic heterostructure consisting of a langatate single crystal with FeBSiC amorphous ferromagnet films deposited on its surface. It was shown that heating of the structure from 220 K to 340 K resulted in a decrease in the quality factor of the acoustic resonance followed by a decrease in the ME coefficient. Annealing the structure in the presence of magnetic field led to an enhancement in the ME coefficient, a decrease in the optimal bias field, and improvement in thermal stability of the ME effect.

Keywords: Magnetolectric effect, Heterostructure, Magnetostriction, Piezoelectricity, Langatate, Amorphous ferromagnet.

1. INTRODUCTION

In recent years, intensive research has been carried out on magnetolectric (ME) effects in composite heterostructures containing ferromagnetic (FM) and piezoelectric (PE) layers [1, 2]. The ME effects manifest themselves in a change in the electric polarization of the structure P in an external magnetic field H (direct effect) or a change in the magnetization of the structure M under the action of an external electric field E (converse effect). The effects arise from a combination of magnetostriction of the FM layer, piezoelectricity in the PE layer and acoustic resonance in the structure. The high efficiency of field conversion makes it possible to use ME effects to elaborate highly sensitive magnetic field sensors, tunable electronic devices, and new data processing elements [3-5].

To create real devices with thermally stable parameters, it is necessary to know the temperature dependence of the characteristics of ME effects in various structures. However, despite the importance of the problem, only a limited number of publications are devoted to this topic. Thus, the temperature characteristics of the ME effect were studied in structures with FM layers of lanthanum-strontium manganite and PE layers of lead zirconate titanate (PZT), manufactured by bonding the layers, laser or magnetron sputtering [6-8]; in structures with a PZT

layer and FM layers of Ni or amorphous ferromagnetic Metglas alloy, manufactured by gluing [9]; in monolithic heterostructures containing a PZT layer or a lanthanum gallium tantalate (LGT) layer with a Ni layer up to 10 μm thick electrolytically deposited on its surface [10, 11]. Analysis of measurement data has shown that the magnitude of the ME effect in structures, as a rule, decreases with increasing temperature due to weakening of the magnetostriction, degradation of the piezoelectric properties of materials, and deterioration of the mechanical properties of the adhesive connection of layers [12].

In this work, we have investigated for the first time the temperature characteristics of the direct ME effect in a monolithic heterostructure containing a single crystal layer of LGT, onto the surface of which Metglas layers are deposited by magnetron sputtering. The choice of LGT as a PE layer is due to its excellent dielectric properties: LGT crystals do not undergo phase transitions up to the melting temperature $T_c \approx 1450^\circ\text{C}$, have low acoustic losses, and lack of hysteresis and pyroelectric effects [13, 14]. The choice of the amorphous ferromagnet Metglas was due to its high magnetostriction and low saturation magnetic field. It was previously shown that LGT-Metglas structures are characterized by high field conversion efficiency. Thus, in the glued heterostructure, the ME coefficient of 720 $\text{V}/(\text{Oe}\cdot\text{cm})$ was obtained at the resonance frequency [15]. In the monolithic heterostructure, the ME coefficient of 76.6 $\text{V}/(\text{Oe}\cdot\text{cm})$ was obtained [16]. All this makes LGT-Metglas structures extremely

*Address correspondence to this author at the MIREA - Russian Technological University, 119454 Moscow, Russia; E-mail: fetisov@mirea.ru

promising for applications and requires detailed studies of their temperature characteristics.

2. EXPERIMENTAL

2.1. Samples

The study used a rectangular plate made of PE lanthanum-gallium tantalate ($\text{La}_3\text{Ga}_{5.5}\text{Ta}_{0.5}\text{B}_{14}$) also known as langate or LGT, on the opposite sides of which FM films were deposited (see Figure 1). The single-crystal LGT X-cut plate was manufactured by Fomos Materials (Moscow, Russia) [17]. The plate had in-plane dimensions of 22 mm x 4.7 mm, a thickness of $a_p = 1.5$ mm, piezoelectric modulus of $d_{11} \approx 5.2$ pC/N, and a relative permittivity of $\epsilon_{11} = 22$ [15, 17]. Amorphous ferromagnetic films (AF) of the composition $\text{Fe}_{77}\text{Co}_4\text{Si}_8\text{B}_{11}$ (Metglas) were deposited using magnetron sputtering on a SUNPLA-40TM setup (Seoul, Republic of Korea). The films were deposited at room temperature, without heating the substrate in an argon atmosphere at a pressure of 0.2 Pa. The magnetron frequency was 13.56 MHz, and the power of 200 W. The film thickness was approximately 2 μm . The FM films were used as electrodes for the PE layer. After measuring the structural, magnetic and ME characteristics of the heterostructure, it was annealed.

Annealing of the structure was carried out in air atmosphere at a temperature of 300 $^\circ\text{C}$ in the presence of dc magnetic field $H=330$ mT, applied along the long side of the structure. The structure was heated from room temperature to 300 $^\circ\text{C}$ for 45 min, held for 30 min, and then slowly cooled. The annealing temperature was chosen to prevent the formation of undesirable phases such as $\alpha\text{-Fe}$ in the Metglas film [18]. X-ray studies performed before and after the annealing showed that the amorphous nature of the Metglas film was preserved.

2.2. Experimental Setup

The block-diagram of the setup used to study ME effects in the heterostructure at various temperatures is shown in Figure 1 [16]. The measurements were carried out using harmonic modulation of the magnetic field. The structure was suspended on thin wires soldered to the centers of the FM films in a dc magnetic field $H = 0\text{-}120$ Oe, directed along its long axis. The field was created using 12 cm diameter Helmholtz coils powered by a TDK Lambda GENH600-1.3 power source. An ac excitation magnetic field $h\cos(2\pi ft)$ with an amplitude up to $h \approx 0.5$ Oe and a frequency of $f = 0\text{-}150$ kHz, was applied parallel to the dc field. The excitation field was created using a second pair of 5 cm diameter Helmholtz coils connected to an Agilent 33210 generator.

The alternating voltage $u(f)$ generated by the structure was taken from the wires and measured using an AKIP 2401 digital voltmeter with an input impedance of 10 M Ω . The voltage spectrum was analyzed using an Agilent E4448A spectrum analyzer. The dc field H was measured with a LakeShore 421 gaussmeter. The amplitude of the alternating field h was determined by monitoring the current through the coils, after they had been calibrated at a frequency of 100 Hz. During the temperature measurements, the structure was placed in a teflon cell and either cooled or heated by flowing gaseous nitrogen through it at a given temperature. The temperature of the nitrogen was changed in steps of 10 $^\circ\text{C}$ steps and maintained with an accuracy of ~ 0.1 $^\circ\text{C}$. The dependences of the voltage amplitude u generated between electrodes of the LGT plate were measured as a function of the dc field H , frequency f , and amplitude h of the excitation field. The installation was controlled using a specialized LabVIEW program on a personal computer.

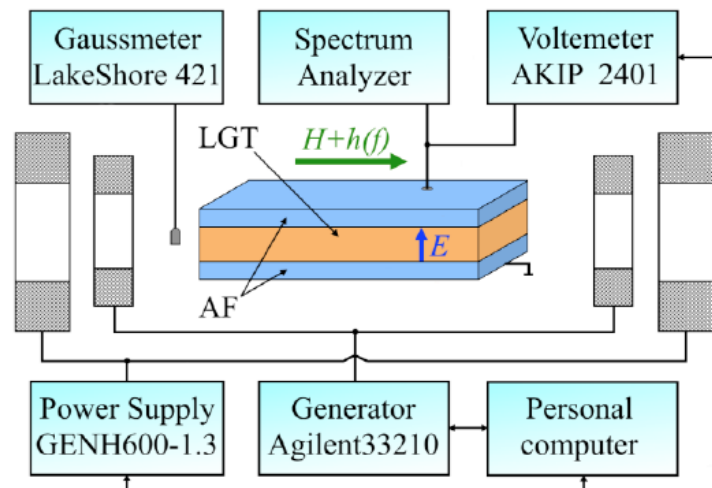


Figure 1: Block-diagram of the experimental setup for the ME effect investigation.

3. MEASUREMENT RESULTS

3.1. ME Effect at Room Temperature

First, the ME effect characteristics in the LGT-Metglas structure were measured at room temperature $T \approx 300$ K and small field h before and after annealing. Figure 2a shows the dependences of the ME voltage u on the excitation magnetic field frequency f with an amplitude of $h=0.22$ Oe, both before and after structure annealing. Before annealing, a resonant peak was observed at a bias field of $H_{m1}=80$ Oe with a central frequency of $f_1=96.531$ kHz, amplitude of $u_1=188$ mV, and a quality factor of $Q_1 \approx 15.6 \cdot 10^3$. After annealing, a peak was observed in the $u(f)$ dependence at a bias field of $H_{m2} \approx 26$ Oe with a central frequency of $f_2=96.517$, an amplitude of $u_2=897$ mV, and a quality factor of $Q_2 \approx 13.8 \cdot 10^3$.

Figure 2b shows the dependences of the peaks amplitude u_1 and u_2 on the dc field H at an excitation field $h=0.22$ Oe before and after annealing the structure. It can be seen that the peak amplitudes are small in weak fields, then grow and reach a maximum at optimal fields, and then smoothly decrease with increasing H . For the original structure, the optimal field at which the generated voltage amplitude is maximum, was $H_{m1} \approx 80$ Oe. After annealing, the optimal bias field decreased to $H_{m2} \approx 26$ Oe. Note the presence of hysteresis in the dependences $u_1(H)$ and $u_2(H)$. The annealing of the structure resulted in a decrease in the coercive field from $H_{c1} \approx 12$ Oe to $H_{c2} \approx 2$ Oe. It was found that the voltages $u_1(H_{m1})$ and $u_2(H_{m2})$ increased linearly as the amplitude of the excitation field increased from zero to $h_{max} \approx 0.7$ Oe. This indicates the linearity of the ME effect.

3.2. Dependence of ME Effect Characteristics on Temperature

At the second stage, the temperature dependences of the ME effect characteristics for both the original and

annealed structures were studied, with temperature changes ranging from 220 to 340 K. Figures 3a and 3b demonstrate the evolution of the amplitude vs. frequency characteristic $u(f)$ of the linear ME effect in the structure before and after annealing, respectively. The curves were measured at the excitation field amplitude $h=0.22$ Oe, the field $H_{m1} \approx 80$ Oe before annealing and $H_{m2} \approx 26$ Oe after annealing. It is clear that as the temperature increases for the initial structure the resonance shifts up in frequency and its amplitude decreases. For the annealed structure, the resonance also shifts up in frequency, but its amplitude remains constant until $T \approx 300$ K, after which it begins to decrease.

Figures 3c and 3d illustrate the evolution of the field dependence of the ME voltages $u_1(H)$ and $u_2(H)$ for the structure both before and after annealing at increasing T . It can be seen that as T increases, the values of the optimal magnetic fields H_{m1} and H_{m2} change and the voltages at these fields $u_1(H_{m1})$ and $u_2(H_{m2})$ decrease.

Based on the measurement results similar to those shown in Figure 3, the temperature dependences of the main characteristics of linear ME effect before and after annealing the structure were constructed, as shown in Figures 4a-d. It is evident that an increase in temperature from 220 K to 340 K led to a gradual increase in the resonance frequency for both original and annealed structures (Figure 4a). The quality factor Q in both cases dropped nearly linearly from $\sim 24 \cdot 10^3$ to $\sim 12 \cdot 10^3$, i.e. by a factor of two (see Figure 4b). The deviations of individual Q values from the linear dependence are associated with errors in measuring Q , which are due to the high quality factor of the resonator. The voltage generated by the structure at the resonant frequency decreased approximately linearly with increasing temperature by $(\Delta u_1 / u_1) 100\% \approx 64\%$ for the original structure and by $(\Delta u_2 / u_2) 100\% \approx 30\%$ for the annealed structure (see Figure 4c). The optimal dc magnetic field corresponding to the maximum ME effect for the original structure remained approximately

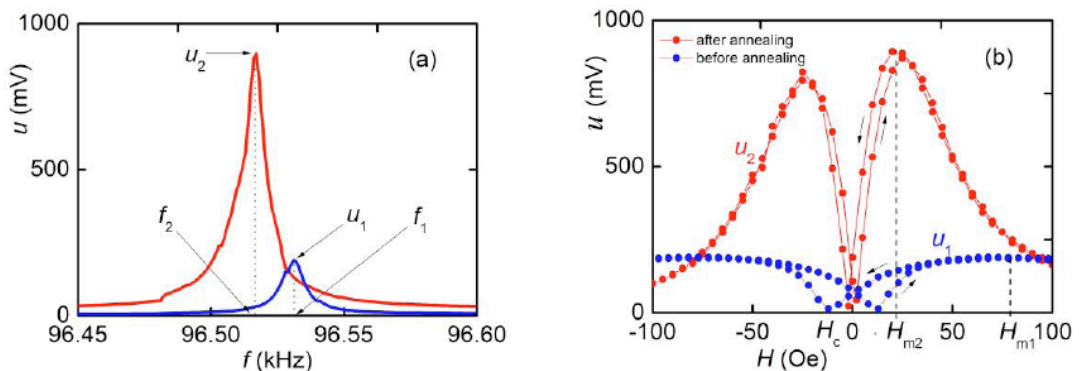


Figure 2: Characteristics of the linear direct ME effect in the LGT-Metglas heterostructure at $T=300$ K before and after annealing: **a)** dependence of the ME voltage u on the excitation field frequency f , **(b)** dependence of the ME voltages u_1 and u_2 at resonant frequencies on the magnetic field H .

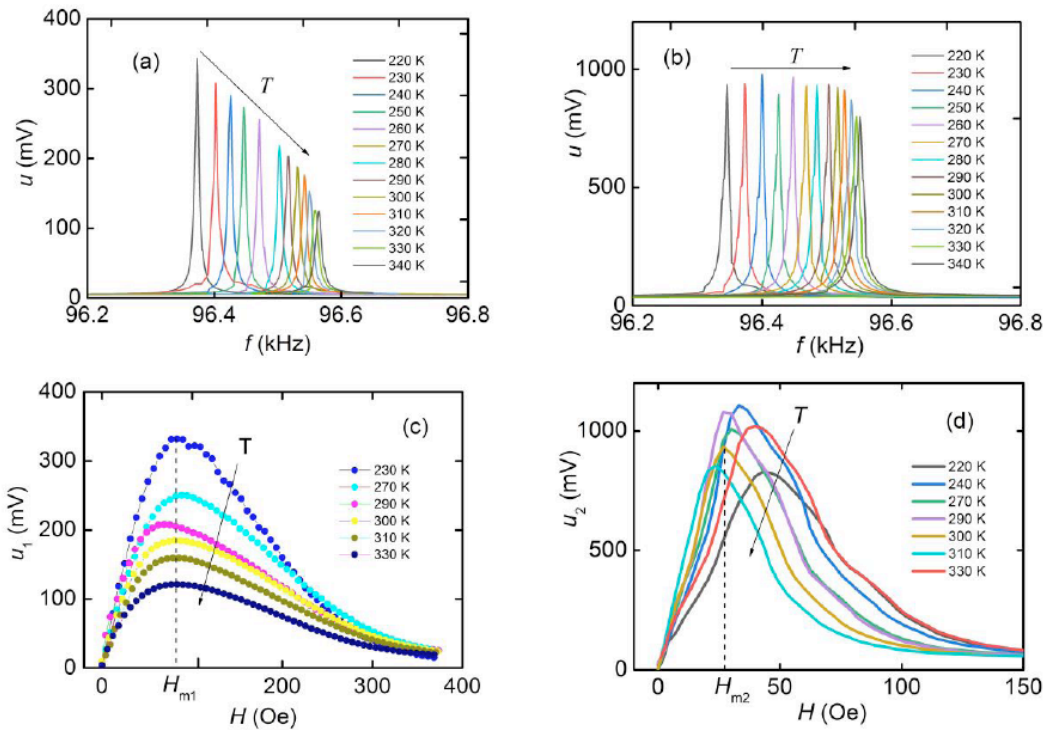


Figure 3: Evolution of frequency and field characteristics of the linear ME effect in the LGT-Metglas heterostructure with increasing temperature: (a) frequency characteristics at $H \approx 80$ Oe before annealing, (b) frequency characteristics at $H \approx 26$ Oe after annealing, (c) field characteristics before annealing, (d) field characteristics after annealing. The field H_{m2} is shown only for the curve at $T=300$ K. Arrows in all figures show the direction of temperature increase.

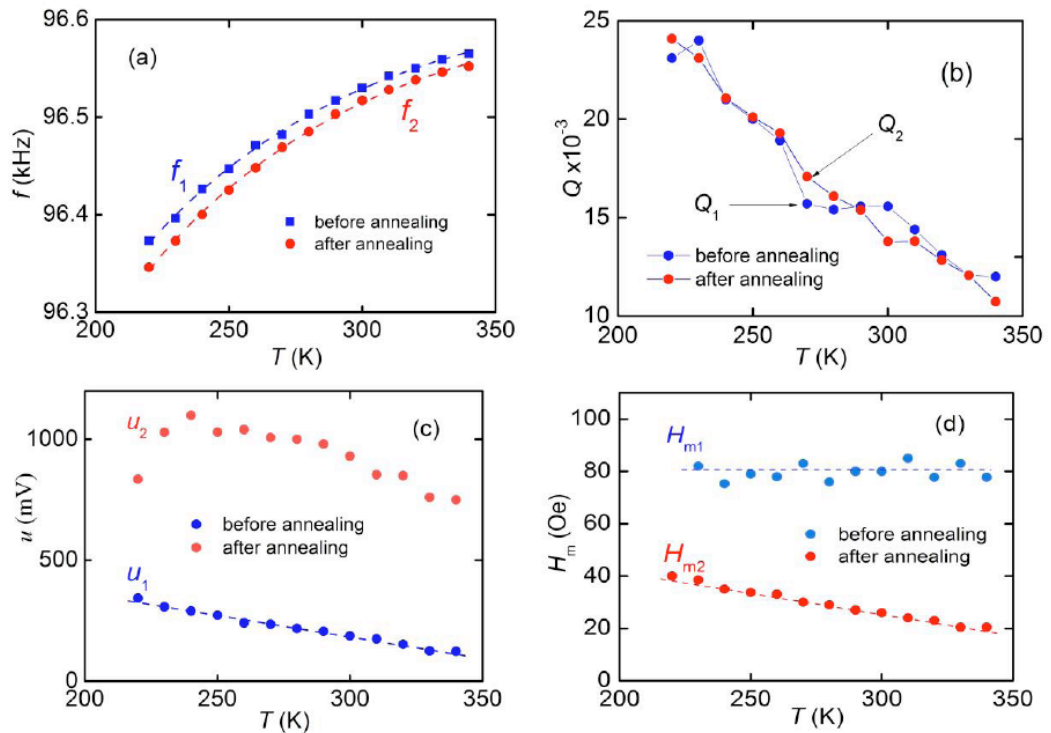


Figure 4: Dependences of the ME effect characteristics in the LGT-Metglas heterostructure on the temperature T before and after annealing: (a) resonant frequencies f_1 and f_2 vs T ; (b) quality factors Q_1 and Q_2 vs T ; (c) ME voltages u_1 and u_2 vs T ; (d) optimal fields H_{m1} and H_{m2} vs T .

constant $H_{m1} \approx 80$ Oe over the entire temperature range, while for the annealed structure it decreased nearly linearly from $H_{m2} \approx 40$ Oe to 20 Oe (Figure 4d).

4. DISCUSSION OF RESULTS

First of all, let's estimate the acoustic resonance frequency of the structure using the formula for the

fundamental mode of planar oscillations of a free rod [19]: $f_r \approx (1/2L)\sqrt{Y/\rho}$, where L is the length of the sample, and Y and ρ are the effective Young's modulus and specific density of the structure, respectively. Since the thickness of the Metglas layers is much smaller than the thickness of the LGT layer, we can neglect their influence on the resonance frequency. Substituting the known values $Y = 110$ GPa, $\rho = 6130$ kg/m³, and $L = 22$ mm for the langatate plate into the formula, we get a resonance frequency of $f_r \approx 100.7$ kHz, which matches the measured value of $f_{1,2} \approx 96.5$ kHz (see Figure 2a).

As follows from Figure 4a, a slight increase in the temperature T led to a small increase in the acoustic resonance frequency of the structure by no more than $\sim 0.22\%$. This is due to the increase in the Young's modulus of the LGT crystal with temperature. In this case, the thin Metglas layers, whose Young's modulus decreases with increasing T , had virtually no effect on the temperature dependence of the resonance frequency. Note the record-high resonant quality factor of the fabricated monolithic heterostructure $Q \approx 25 \cdot 10^3$, which is almost an order of magnitude higher than the quality factor for glued structures $\sim (2 \dots 4) \cdot 10^3$ [12]. The high quality factor is achieved due to small thickness of the FM layers and indicates good quality of mechanical contact between layers of the structure. The decrease in the quality factor for the monolithic heterostructure (Figure 4b) with increasing T , as in glued heterostructures, is due to an increase in acoustic losses in LGT crystal caused by the phonon-phonon interaction and inelastic scattering on dislocations [20]. It is evident that the annealing of the Metglas layers had virtually no effect on the resonant quality factor.

Using the data in Figure 4c, one can estimate the change in the ME coefficient of the structure $\alpha_E = u / (a_p h)$ (where u is the amplitude of the electrical voltage generated between the electrodes of a PE layer of thickness a_p under the influence of an alternating magnetic field of amplitude h) with increasing temperature. The ME coefficient for the original structure decreased nearly linearly from $\alpha_{E1} = u_1 / (a_p h) \approx 11.4$ V/(Oe cm) to 3.8 (V/Oe cm), i.e. by $\sim 66\%$, and for the annealed structure it decreased from $\alpha_{E2} \approx u_2 / (a_p h) \approx 33$ V/(Oe cm) to 23 (V/Oe cm), i.e. by $\sim 30\%$. The obtained ME coefficient for the original structure is comparable with the coefficient of ~ 8.3 V/(Oe cm) for the glued LGT-Metglas structure with a 20 μm thick Metglas layer [10]. However, this coefficient turned out to be less than that achieved in a monolithic structure of similar composition [16], as we used a thicker LGT layer

The most impressive result of annealing the monolithic LGT-Metglas heterostructure is the enhancement in the ME coefficient and the decrease in

the optimal dc bias magnetic field H_m . To understand the reason for this, we measured the magnetization curves of the structure both before and after annealing, which are shown in Figure 5. The curves were obtained using the longitudinal Kerr effect method at a wavelength of 0.628 μm . The dc magnetic field was applied in the plane of the structure along its long side. As a result of annealing, the saturation field of the Metglas layers H_s decreased from ~ 300 Oe to ~ 100 Oe. The coercive field H_c also decreased from ~ 25 Oe to ~ 9 Oe. Additionally, there was an increase in the slope of the magnetization curve $\partial M / \partial H$ (i.e., the magnetic permeability) in the low-field region.

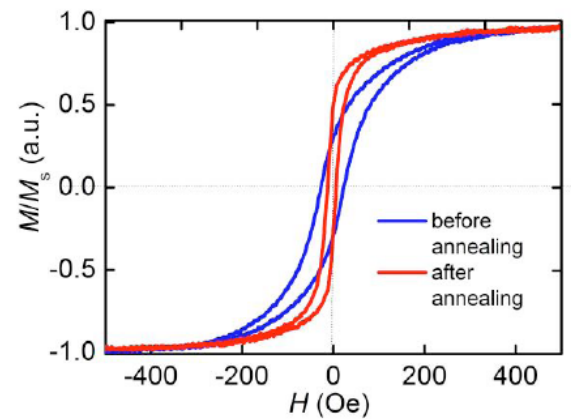


Figure 5: Dependence of the relative magnetization M/M_s of the LGT-Metglas heterostructure on the magnetic field H before and after annealing.

When Metglas was deposited on the LGT surface, mechanical stresses appeared in the film. Annealing relieved these stresses and energy losses due to domain wall rearrangement, and, as a result, increased the magnetic permeability of the FM layers. The value of the ME coefficient in composite FM-PE heterostructures is proportional to the product of the piezoelectric modulus d of the PE layer and the piezomagnetic modulus $q = \partial \lambda / \partial H|_H$ of the FM layer [21]. Since the magnetostriction in low fields depends quadratically on the magnetization, $\lambda \sim M^2$, we obtain the expression for the piezomagnetic modulus of the FM layer $q(H) \sim \partial M^2 / \partial H|_H \sim 2M(\partial M / \partial H|_H)$ [22]. This implies that an increase in the magnetic permeability leads to an increase in both piezomagnetic modulus q and ME coefficient of the structure. It should be noted that an enhancement of the ME effect after annealing has been previously observed in structures of other compositions containing Metglas layers [18, 23].

Thus, the results of the studies demonstrated changes in the characteristics of the ME effect in the LGT-Metglas monolithic heterostructure with increasing temperature, which must be taken into account when developing methods for thermal stabilization of ME devices.

5. CONCLUSION

In summary, the characteristics of resonant ME effect in the monolithic LGT-Metglas heterostructure in the temperature range of $T=220\text{...}340$ K are investigated. It is shown that heating the structure significantly affects characteristics of the ME effect. With increasing T , the acoustic resonance frequency increased by no more than 0.2%, but the resonance quality factor dropped from $Q\approx 24\cdot 10^3$ by a factor of two. This led to a monotonic decrease in the ME coefficient from $\alpha_E \approx 11.4$ V/(Oe·cm) to 3.8 (V/Oe·cm). Annealing the structure in the presence of dc magnetic field led to an enhancement of the ME effect characteristics. The maximum ME coefficient increased up to ~ 33 V/(Oe cm), and the optimal bias magnetic field decreased from ~ 80 Oe to ~ 25 Oe. The research results can be useful in developing methods for thermal stabilization of the ME effect characteristics in monolithic heterostructures.

ACKNOWLEDGEMENTS

The research was supported by the Russian Ministry of Science and Education within the framework of the State Assignment for Universities (No. FSFZ-2023-0005) and by the National Natural Science Foundation of China (grant No. 12474083). Kubasov I., Turutin A. and Temirov A. are grateful for the support from the Russian Science Foundation (grant No. 24-49-10017) regarding the synthesis of $\text{Fe}_{77}\text{Co}_4\text{Si}_8\text{B}_{11}$ films, the preparation and annealing of magnetoelectric samples.

CONFLICTS OF INTEREST

The authors have no conflicts of interest.

REFERENCES

- [1] Nan CW, Bichurin MI, Dong S, Viehland D, Srinivasan G. Multiferroic magnetoelectric composites: historical perspective, status and future direction., J. Appl. Phys. 2008; 103: 031101. <https://doi.org/10.1063/1.2836410>
- [2] Fetisov YK, Srinivasan G. Nonlinear magnetoelectric effects in layered multiferroic composites. J Appl. Phys. 2024; 135: 024102. <https://doi.org/10.1063/5.0183351>
- [3] Turutin AV, Kubasov IV, Kislyuk AM et al. Ultra-sensitive magnetoelectric sensors of magnetic fields for biomedical applications. Nanotechnol. Russia. 2022; 17: 261-289. <https://doi.org/10.1134/S2635167622030223>
- [4] Palneedi H, Annapureddy V, Priya S, Ryu J. Status and perspectives of multiferroic magnetoelectric composite materials and applications. Actuators. 2016; 5: 9. <https://doi.org/10.3390/act5010009>
- [5] Hu JM, Nan CW. Opportunities and challenges for magnetoelectric devices. APL Mater. 2019; 7: 080905. <https://doi.org/10.1063/1.5112089>
- [6] Zhang N, Srinivasan G, Balbashov AM. Low-frequency magnetoelectric interactions in single crystal and polycrystalline bilayers of lanthanum strontium manganite and lead zirconate titanate. J. Mater. Sci. 2009; 44: 5120. <https://doi.org/10.1007/s10853-009-3455-2>
- [7] Li T, Wang H, Hu Z, Li K. Temperature dependence of magnetoelectric coupling in $\text{La}_{0.7}\text{Sr}_{0.3}\text{MnO}_3/\text{BaTiO}_3$ layered heterostructure with various volume fractions. Thin Solid Films. 2016; 616: 1-5. <https://doi.org/10.1016/j.tsf.2016.07.071>
- [8] Vaz CAF, Segal Y, Hoffman J, Grober RD, Walker FJ, Ahn CH. Temperature dependence of the magnetoelectric effect in $\text{Pb}(\text{Zr}_{0.2}\text{Ti}_{0.8})\text{O}_3/\text{La}_{0.8}\text{Sr}_{0.2}\text{MnO}_3$ multiferroic heterostructures. Appl. Phys. Lett. 2010; 97: 042506. <https://doi.org/10.1063/1.3472259>
- [9] Fang F, Xu YT, Yang W. Magnetoelectric coupling of laminated composites under combined thermal and magnetic loadings. J. Appl. Phys. 2012; 111: 023906. <https://doi.org/10.1063/1.3677945>
- [10] Burdin DA, Fetisov YK, Chashin DV, Ekonomov NA. Temperature characteristics of magnetoelectric interaction in langatate-ferromagnet composite resonators. Bull. Russian Acad. Sci. Phys. 2014; 78: 131-133. <https://doi.org/10.3103/S1062873814020105>
- [11] Burdin D, Chashin D, Ekonomov N, Fetisov Y. Temperature characteristics of magnetoelectric effect in bilayer ferromagnetic-piezoelectric structures, Solid State Phen. 2015; 233-234: 357-359. <https://doi.org/10.4028/www.scientific.net/SSP.233-234.357>
- [12] Burdin DA, Ekonomov NA, Chashin DV, Fetisov LY, Fetisov YK, Shamonin M. Temperature dependence of the resonant magnetoelectric effect in layered heterostructures. Materials. 2017; 10: 1183. <https://doi.org/10.3390/ma10101183>
- [13] Pisarevsky YV, Senyushenkov PA, Mill BV, Moiseeva NA. Elastic, piezoelectric, dielectric properties of $\text{La}_3\text{Ga}_{5.5}\text{Ta}_{0.5}\text{O}_{14}$ single crystals. Proc. of the 1998 IEEE International Frequency Control Symp. (Cat.No.98CH36165). 1998; p.742-747. <https://doi.org/10.1109/FREQ.1998.717982>
- [14] Shi X, Yuan D, Yin X, Wei A, Guo S, Yu F. Crystal growth and dielectric, piezoelectric and elastic properties of $\text{Ca}_3\text{TaGa}_3\text{Si}_2\text{O}_{14}$ single crystal. Solid State Comm. 2007; 142(3): 173-176. <https://doi.org/10.1016/j.ssc.2007.01.047>
- [15] Sreenivasulu G, Fetisov LY, Fetisov YK, Srinivasan G. Piezoelectric single crystal langatate and ferromagnetic composites: Studies on G.low-frequency and resonance magnetoelectric effects. Appl. Phys. Lett. 2012; 100: 052901. <https://doi.org/10.1063/1.3679661>
- [16] Fetisov LY, Dzhaparidze MV, Savelev DV et al. Magnetoelectric effect in amorphous ferromagnetic FeCoSiB /Langatate monolithic heterostructure for magnetic field sensing. Sensors. 2023; 23: 4523. <https://doi.org/10.3390/s23094523>
- [17] FOMOS Materials. Available online: <https://en.newpiezo.com/> (accessed on 17 March 2025).
- [18] Freeman E, Harper J, Goel N, et al. Improving the magnetoelectric performance of Metglas/PZT laminates by annealing in a magnetic field, Smart Mater. Struct. 2017; 26: 085038 <https://doi.org/10.1088/1361-665X/aa770b>
- [19] Timoshenko S. Vibration Problems in Engineering. Toronto: D. Van Nostrand Company Inc. 1955.
- [20] Johnson W, Kim S, Lauria D. Anelastic loss in langatate. Proc. 2000 IEEE/EIA International Conf. 2000; 186-190. <https://doi.org/10.1109/FREQ.2000.887351>
- [21] Fetisov LY, Chashin DV, Fetisov YK, Segalla AG, Srinivasan G. Resonance magnetoelectric effects in a layered composite under magnetic and electrical excitations Journal of Applied Physics, 2012; 112(1): 014103 <https://doi.org/10.1063/1.4733466>
- [22] Fetisov YK, Chashin DV, Ekonomov NA, Burdin DA, Fetisov LY. Correlation between magnetoelectric and magnetic properties of ferromagnetic-piezoelectric structures. IEEE Trans. Magn. 2015; 51(11): 2503403. <https://doi.org/10.1109/TMAG.2015.2443031>

[23] Grechishkin RM, Kaplunov IA, Ilyashenko SE *et al.*
Magnetolectric effect in Metglas/ piezoelectric macrofiber

composites, *Ferroelectrics*. 2011; 424(1): 78-85.
<https://doi.org/10.1080/00150193.2011.623939>

Received on 22-02-2025

Accepted on 18-03-2025

Published on 26-03-2025

<https://doi.org/10.31875/2410-4701.2025.12.01>

© 2025 Bolotina *et al.*

This is an open-access article licensed under the terms of the Creative Commons Attribution License (<http://creativecommons.org/licenses/by/4.0/>), which permits unrestricted use, distribution, and reproduction in any medium, provided the work is properly cited.